Breast Cancer Res Treat (2012) 132:75–85
DOI 10.1007/s10549-011-1534-y

PRECLINICAL STUDY

Prolonged mammosphere culture of MCF-7 cells induces an EMT and repression of the estrogen receptor by microRNAs

I. K. Guttilla · K. N. Phoenix · X. Hong · J. S. Tirnauer · K. P. Claffey · B. A. White

Received: 10 February 2011 / Accepted: 16 April 2011 / Published online: 7 May 2011

Abstract Mammosphere culture has been used widely for the enrichment of mammary epithelial stem cells and breast cancer stem cells (CSCs). Epithelial-to-mesenchymal transition (EMT) also induces stem cell features in normal and transformed mammary cells. We examined whether mammosphere culture conditions per se induced EMT in the epithelial MCF-7 breast cancer cell line. MCF-7 cells were cultured as mammospheres for 5 weeks, with dispersal and reseeding at the end of each week. This mammosphere culture induced a complete EMT by 3 weeks. Return of the cells to standard adherent culture conditions in serum-supplemented media generated a cell population (called MCF-7_M cells), which displays a stable mesenchymal and CSC-like $CD^{44+}/CD^{24-/low}$ phenotype. EMT was accompanied by a stable, marked increase in EMT-associated transcription factors and mesenchymal markers, and a decrease in epithelial markers and estrogen receptor α (ERα). MCF-7_M cells showed increased motility, proliferation and chemoresistance in vitro, and produced larger tumors in immunodeficient mice with or without estrogen supplementation. MicroRNA analysis showed suppression of miR-200c, miR-203, and miR-205; and increases in miR-222 and miR-221. Antisense hairpin RNA inhibitor targeting miR-221 resulted in re-expression of ERα in MCF-7_M cells. This study provides the first example of mammosphere culture conditions inducing EMT and of EMT regulating microRNAs that target ERα.

Keywords Breast cancer · EMT · Stem cells · Estrogen receptor alpha · MicroRNAs

Electronic supplementary material The online version of this article (doi:10.1007/s10549-011-1534-y) contains supplementary material, which is available to authorized users.

I. K. Guttilla · K. N. Phoenix · X. Hong · K. P. Claffey · B. A. White (✉)
Department of Cell Biology, University of Connecticut Health Center, Farmington, CT 06030-3505, USA
e-mail: bwhite@nso2.uchc.edu

J. S. Tirnauer
Center for Molecular Medicine, University of Connecticut Health Center, Farmington, CT 06030, USA

J. S. Tirnauer · K. P. Claffey
NEAG Comprehensive Cancer Center, University of Connecticut Health Center, Farmington, CT 06030, USA

K. N. Phoenix · X. Hong · K. P. Claffey
Center for Vascular Biology, University of Connecticut Health Center, Farmington, CT 06030-6501, USA

K. P. Claffey (✉)
Breast Cancer Research Program, NEAG Comprehensive Cancer Center, University of Connecticut Health Center, Farmington, CT 06030-6501, USA
e-mail: claffey@nso2.uchc.edu

Introduction

"Luminal A" represents the predominant form of invasive breast cancer (IBC) and expresses ERα GATA3 and FOXA1, [1, 2]. Luminal A cells also display hallmarks of epithelial organization, including intercellular junctional complexes and apico-basal polarity. Luminal A cells are poorly invasive or metastatic, resulting in a more favorable prognosis in most patients [1, 2].

Nevertheless, Luminal A tumors can progress to higher grades and metastasize. This progression is likely driven by a subset of cells that shed epithelial constraints and acquire an invasive, mesenchymal phenotype through the process

of type 3 epithelial-to-mesenchymal transition [3–8]; referred to herein as EMT. A broad range of extracellular factors induces EMT, including growth factors, inflammatory cytokines, hypoxia, and cell–matrix interactions. EMT is driven by several transcription factors, including members of the Snail, Twist, and Zeb families. EMT results in diminished expression of junctional proteins (e.g., E-cadherin), loss of apico-basal polarity, and the acquisition of a mesenchymal phenotype with back/front polarity and vimentin expression. In addition, EMT results in increased invasiveness and is likely an antecedent to metastasis.

EMT confers another unwelcome trait to IBC cells—expansion of the cancer stem cell (CSC) fraction [9–12]. The CSC subpopulation retains tumorigenic and self-renewal potential and is relatively insensitive to anti-tumor therapies [10]. Thus, EMT increases cancer metastasis and the probability of recurrence. EMT has recently become the object of intense scrutiny, and the molecular components of EMT might serve as prognostic markers and represent high-impact therapeutic targets in IBC.

Several epithelial/luminal-promoting factors that antagonize EMT in Luminal IBC have been identified. ERα opposes EMT by suppressing Snail 1 and Snail 2 (Slug) [13, 14]. ERα stimulates GATA3 expression [15], which opposes EMT [16, 17]. ERα also interacts with FOXA1 [15], which inhibits EMT in pancreatic cancer [18]. Thus, ERα, GATA3, and FOXA1 appear to be pivotal in maintaining epithelial differentiation in Luminal IBC, in part by providing a molecular firewall to EMT progression. This raises the possibility that anti-estrogen therapies, while reducing the bulk of Luminal A tumors, might degrade safeguards against EMT. In fact, recurrent IBC in Letrozole-treated patients exhibited the mesenchymal, CSC-related, Claudin-low phenotype [19].

A second recently discovered mechanism that maintains epithelial differentiation and opposes EMT comprises several microRNAs, including the miR-200 family, miR-203, and miR-205 [20–22]. These microRNAs target mRNAs encoding the EMT effectors Zeb1 and Zeb2. Thus, ERα suppresses transcription of EMT effectors, while microRNAs provide a post-transcriptional block. This model also includes several double-negative feedback loops, by which EMT effectors suppress transcription of ERα and genes encoding EMT-opposing microRNAs [23]. EMT effectors also probably cooperate with EMT-promoting microRNAs, whose expression is increased during EMT. This is particularly likely for ERα, which is also targeted by several microRNAs [24]. However, the identity of ERα-targeting microRNAs during EMT remains undetermined.

Mammosphere culture has been utilized to enrich for normal adult stem cells and for CSCs [25, 26]. Since both mammosphere culture and EMT expand the CSC fraction, we examined whether mammosphere culture could induce an EMT. We demonstrate that prolonged serial mammosphere culture of ERα-positive MCF-7 cells results in a persistent EMT, with the expression of microRNAs that target ERα mRNA.

Materials and methods

Cell culture and drug treatments

MCF-7 and MDA-MB-231 breast carcinoma cells (ATCC, Manassas, VA) were propagated in DMEM/F12, 10% fetal bovine serum (FBS), 1% penicillin/streptomycin (Gibco, Carlsbad, CA). For mammosphere culture, MCF-7 cells were seeded at 2.5×10^4 cells/ml in 6-well Ultralow Adherence plates (Corning Inc., Corning, NY) in DMEM/F12 with 5 μg/ml bovine insulin (Sigma, St. Louis, MO), 20 ng/ml recombinant epidermal growth factor (Sigma-Aldrich), 20 ng/ml basic fibroblast growth factor (Gibco), 1× B27 supplement (Invitrogen, Carlsbad, CA), 0.5 μg/ml cortisol (Sigma), and 1% penicillin/streptomycin (Gibco), as described in [26]. Prolonged mammosphere culture was achieved using weekly trypsinization and dissociation with a 21-gauge needle followed by reseeding in mammosphere media at 2.5×10^4 cells/well into Ultralow Adherence 6-well plates. Each generation was designated by the week of culture in mammosphere media (M1, M2, etc.).

Cells were treated with Docetaxel or Tamoxifen (Sigma) at the noted concentrations and durations. Docetaxel-treated cells were cultured in regular growth medium (RGM). Tamoxifen-treated cells were cultured in hormone-depleted medium (HDM) (phenol-red free DMEM/F12 with 10% charcoal-dextran treated FBS, and 1% penicillin/streptomycin) (Gibco). Cell viability was assayed by trypan blue staining done in triplicate in three independent experiments.

cDNA synthesis and endpoint PCR

Total RNA was isolated using Trizol Reagent (Invitrogen, Carlsbad, CA) and reverse transcribed using 250 ng random hexamers (or 2 pmol of a gene-specific primer) according to directions for Superscript III (Invitrogen). In general, 2 μl of cDNA was amplified in standard PCR reactions and detected by standard methods. Primer sequences are listed in Supplemental Table 1.

Semi-quantitative endpoint PCR analysis of mature microRNAs

Mature microRNAs were detected by RT-PCR using a stem-loop gene-specific primer for reverse transcription

[27]. For cDNA synthesis, 1 μg of total RNA, 2 pmol gene-specific primer, and 0.5 mM of dNTPs were incubated at 65°C for 5 min. Superscript™ III Reverse Transcriptase (100 units; Invitrogen, Carlsbad, CA) and Kit reagents were added (final volume 20 μl) and incubated at 55°C for 60 min, followed 70°C for 15 min. PCR was performed with 0.2 μM primers, and 2 μl cDNA in 50 μl, using 95°C/5 min; 95°C/30 s, 55°C/30 s, 72°C/30 s for 30 cycles. Products were resolved on 10% nondenaturing acrylamide gels, stained, and imaged. Primer sequences are listed in Supplemental Table 2. miR-98 was used as a loading control, as its levels were constant in all samples (i.e., MCF-7 cells, early and late mammospheres, and MCF-7_M cells).

Western blotting

Cell lysates were processed for standard Western blotting. Primary antibodies to ERα and GAPDH (Abcam Inc., Cambridge, MA) were diluted in 5% milk/TBST and incubated overnight at 4°C (GAPDH 1:10,000 and ERα 1:1000). IgG horseradish peroxidase-conjugated secondary antibody (Santa Cruz Biotechnology, Inc., Santa Cruz, CA) was diluted 1:5000. Blots were processed for enhanced chemiluminescence and exposed to chemiluminescence film (Eastman Kodak Company, Rochester, NY).

Immunofluorescence and microscopy

Images of adherent MCF-7 parental cells and MCF-7_M cells were taken using a Zeiss Axio Observer A1 microscope at 10×. Images of non-adherent mammospheres were taken using a Zeiss Pascal microscope at 40× with a NA 1.2 water immersion objective. Immunofluorescence was done in cells grown on glass coverslips and fixed in ice-cold methanol for 5 min. Primary antibodies were used against E-cadherin (Santa Cruz Biotechnology, Santa Cruz, CA) and vimentin (Thermo Scientific, Fremont, CA), with Alexa-conjugated secondary antibodies (Invitrogen). Chromatin was stained with DRAQ5 (Biostatus, Leicestershire, UK). Imaging was performed with a TE2000-U microscope (Nikon Instruments, Melville, NY) using a Yokogawa CSU-10 spinning disk confocal head (Perkin Elmer, Wellesley, MA) and an Orca AG CCD camera (Hamamatsu Photonics, Bridgewater, NJ). Image acquisition and analysis were controlled by MetaMorph software (Molecular Devices Corp., Sunnyvale, CA).

Scratch wound and cell motility assays

Scratch wounds were made with a p200 pipette tip on confluent cells on glass coverslips. Coverslips were sealed in modified Rose chambers using pre-equilibrated media, and wound closure was imaged by phase contrast at 20× magnification using shuttered light at 15 min intervals; temperature was maintained at 36°C by an air curtain incubator (ASI 400; Nevtek, Burnsville, VA). Three independent migration assays were performed for each cell line.

Flow cytometry

MCF-7, MDA-MB-231, and MCF-7_M cells were trypsinized, washed in 0.1% BSA in PBS, counted, and resuspended in 2% FBS/0.01% NaN_3 at 1×10^6/100 μl. Cells were labeled with CD24-PE (BD Biosciences, Mississauga, ON, Canada; 555428) and CD44-FITC (BD Biosciences; 555478), and incubated at 4°C according to the supplier's protocol. Cells were washed, fixed in PBS with 10% formalin, and analyzed on a FACSCalibur (BD Biosciences). Unstained or single antibody-stained cells were analyzed for each cell line.

MicroRNA expression array

Human Cancer RT^2 microRNA PCR arrays were obtained from SA Biosciences (Frederick, MD). RNA was isolated from adherent MCF-7 cells, M2 and M4 mammospheres, and MCF-7_M cells by Trizol. cDNA was synthesized using the RT^2 microRNA First Strand Kit (SA Biosciences) from 1 μg of total RNA. PCR arrays were run on an Applied Biosystems 7900 HT Fast Real-time PCR system according to the manufacturer's protocol (Applied Biosystems, Carlsbad, CA). Data was analyzed using online software at SA Biosciences (http://pcrdataanalysis.sabiosciences.com/pcr/arrayanalysis.php).

AntagomiR treatments

MCF-7_M cells were transfected with miRIDIAN™ microRNA Hairpin Inhibitor (Dharmacon/Thermo Fisher Scientific, Lafayette, CO) directed against miR-221 (40 nM) in 12-well plates. Inhibitor was combined with OPTI-MEM® (Invitrogen, Carlsbad, CA) and 2 μl Lipofectamine 2000 (Invitrogen) per sample in a volume of 100 μl for 20 min and added to cells in 400 μl of OPTI-MEM®. Cells were incubated for 4 h, after which time antibiotic-free media was added, and cells harvested 24 h later.

Mouse tumor xenografts

MCF-7 and MCF-7_M cells were harvested with trypsinization, resuspended in DMEM, and mixed with Matrigel (BD Biosciences, Mississauga, ON, Canada) to obtain 5×10^5 cells in 250 μl, and injected into two subcutaneous mammary fat pad sites on SCID mice implanted with 90-day slow-release estradiol pellets (Innovative Research

of America, Inc.) or sham implanted for estradiol-negative animals ($n = 10$/group). Tumors were allowed to grow for 21 days (MCF-7_M tumors) or 42 days (MCF-7 tumors) and measured with external calipers. At the indicated time points, tumors were harvested and weighed. Histological and immunohistological analyses for E-cadherin, cleaved Caspase-3, and Ki67 were performed as described previously [28].

Results

Serial mammosphere culture of MCF-7 cells induces EMT

In prolonged mammosphere culture of MCF-7 cells, we observed that tightly adherent spheroids switched to loosely aggregated spheroids (Fig. 1a). Upon transfer back to adherent flasks, cells from the M5 aggregates showed reduced cell–cell interactions and a fibroblastic morphology (Fig. 1a). The reduction in cell–cell adhesion was paralleled by a marked decrease in E-cadherin expression and a gain in vimentin expression (Fig. 1b), two classic features of EMT. This phenotype was stable in culture for at least ten cell passages. The EMT cells were designated as MCF-7_M to highlight their mesenchymal properties.

We next tested functional characteristics of the EMT, including migration and proliferation rates. In scratch wound assays, the parental MCF-7 cells migrated into the wound at an average rate of 4.9 microns/h, often failing to close the wound after 24 h (Fig. 1c). In contrast, MCF-7_M cells migrated rapidly, with a mean rate of 10.6 microns/h. Interestingly, MCF-7_M cells demonstrated spontaneous non-directional migration, which was not observed in the parental MCF-7 cells (not shown).

To assess proliferation, equal numbers of MCF-7 and MCF-7_M cells were plated, and viable cells counted after 96 h. The number of MCF-7_M cells was approximately threefold higher than MCF-7 cells in either RGM or HDM (Fig. S1). Thus, MCF-7_M cells display increased migratory capacity and proliferation rate compared to MCF-7 cells.

MCF-7_M cells show EMT-related changes in gene expression

EMT typically involves changes in gene expression [7, 20, 21, 29]. To test this, we assayed the expression of luminal breast cancer, mesenchymal breast cancer, and EMT genes in parental MCF-7 cells, M1 through M4 mammospheres, and MCF-7_M cells. This showed that luminal-associated gene expression was progressively suppressed in the M1 and M2 mammospheres; conversely, mesenchymal-associated mRNA expression was induced in M2–M4 samples (Fig. 2a, b). There was also a striking increase in the expression of four EMT-related transcriptional factors: Snail 1 and Slug (Fig. 2c), and ZEB1 and ZEB2 (Fig. 2d). We also observed expression of the inflammatory cytokine interleukin-6 (IL-6) and the receptor tyrosine kinase Axl (Fig. 2c, d), both of which have been shown to induce EMT in MCF-7 cells [30, 31]. The enhanced expression of ZEB1, ZEB2 and AXL in MCF-7_M cells (Fig. 2d) suggests the acquisition of a mesenchymal and stem cell-associated "Basal B" phenotype [32].

MCF-7_M cells display the CSC-associated $CD44^+/CD24^{-/low}$ phenotype and chemoresistance

Mammosphere culture and EMT enrich for a $CD44^+/CD24^{-/low}$ stem cell phenotype in normal mammary epithelial and breast cancer cells [9, 10, 33, 34]. Thus, we compared CD44/CD24 expression in MCF-7 and MCF-7_M cells. The majority of MCF-7 cells sorted into the $CD44^{low}/CD24^{hi}$ fraction, whereas most MCF-7_M cells sorted into the $CD44^+/CD24^{low/-}$ fraction, consistent with a CSC phenotype (Fig. 3a).

Resistance to cytotoxic chemotherapy has also been associated with both EMT and CSCs [10]. We tested chemotherapy resistance in MCF-7 and MCF-7_M cells, and found that while MCF-7 cells showed a 60% decrease in viability after treatment with Docetaxel for 24 h, MCF-7_M cells only showed a 20% decrease in viability (Fig. 3b). MCF-7_M cells were also insensitive to tamoxifen. Whereas, 10 μM tamoxifen decreased the growth rate of MCF-7 cells by 58%, MCF-7_M cells showed no growth reduction (Fig. 3c).

MCF-7_M cells are highly tumorigenic

We performed orthotopic injection of cells into the mammary fat pad of athymic nude mice to assess the degree of tumorigenicity and the stability of the MCF-7_M cell mesenchymal phenotype in vivo. While the parental MCF-7 cells took more than 40 days to expand beyond the Matrigel plug, and required estradiol supplementation to do so, MCF-7_M cells exceeded the plug by 3 weeks, and their growth was estradiol independent (Fig. 4a). MCF-7_M-derived tumors were at least double the weight of parental MCF-7 tumors with estradiol and nearly five times the weight of parental tumors without estradiol (Fig. 4b).

To assess the stability of the EMT in vivo, tumors were excised and immunohistochemistry performed. This showed abundant E-cadherin in parental MCF-7 cell-derived tumors, with marked reduction in MCF-7_M-derived tumors (Fig. 4d). By RT-PCR, MCF-7 cell-derived tumors displayed robust ERα, E-cadherin, and GATA-3 mRNA

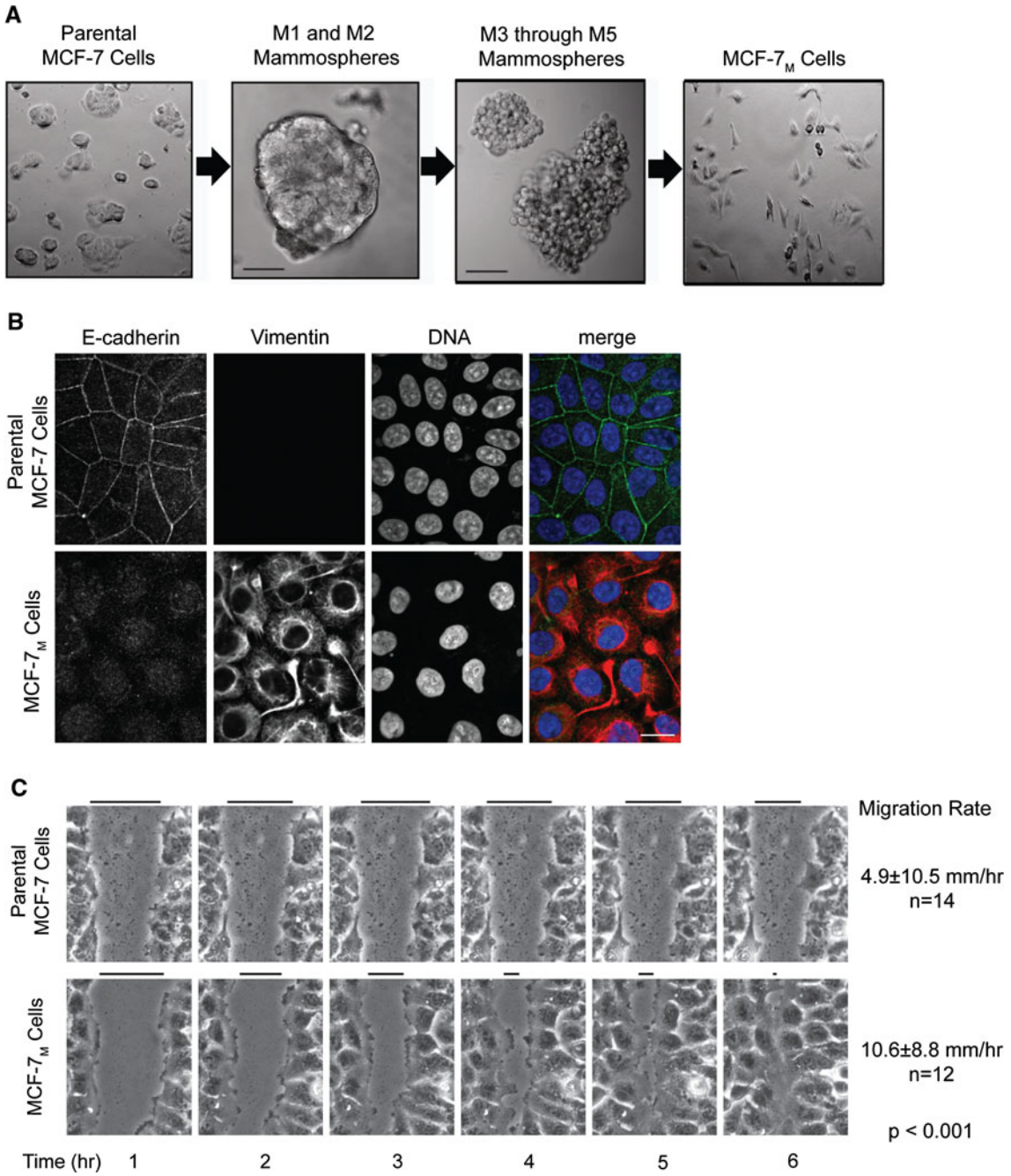

Fig. 1 MCF-7 cells cultured as mammospheres undergo a stable EMT. **a** Morphological changes. Images of MCF-7 parental cells grown as monolayers (*left*), stages of spheroid culture that are representative of M1 and M2 mammospheres, and M3 through M5 mammospheres (*center panels*) and MCF-7_M cells as monolayers (*right*), showing progressive loss of cell cohesion. This phenomenon was observed in four independent experiments over the course of several months. **b** Loss of E-cadherin and gain of vimentin expression. Immunofluorescence shows that parental MCF-7 cells express E-cadherin at cell–cell junctions and do not express vimentin. MCF-7_M cells show lack of E-cadherin and gain of vimentin. **c** Gain of migratory ability. Representative panels from a scratch wound assay imaged by time-lapse microscopy show slow migration of MCF-7 cells with failure to close the wound by 6 h, whereas MCF-7_M cells migrate faster and completely fill the wound. *Black lines* above panels show size of the remaining wound. Data are representative of three independent experiments. *Scale bars* 50 μm in (**a**) and 20 μm in (**b**)

expression, while MCF-7_M cell-derived tumors were devoid of luminal marker gene expression, and displayed significant levels of EGF receptor and vimentin mRNAs (Fig. 5).

To assess the mechanism of increased growth of MCF-7_M tumors, cell proliferation and apoptosis were evaluated using Ki67 and cleaved caspase-3 immunostaining (Fig. 4e–g). There were no significant differences in Ki67

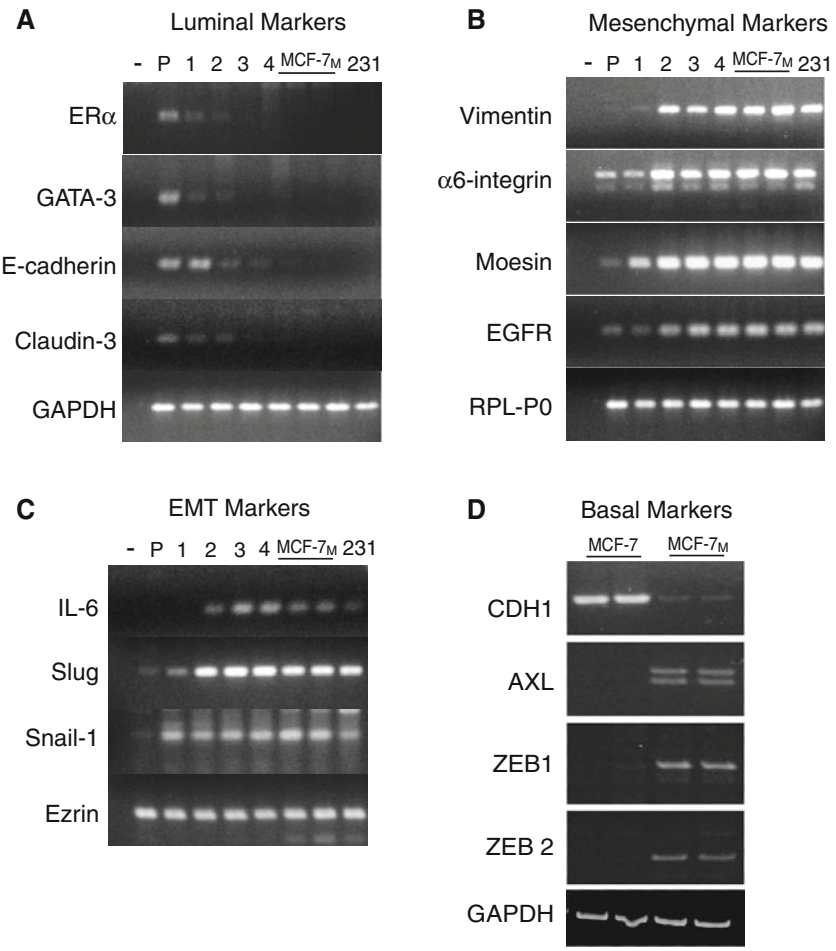

Fig. 2 Messenger RNA expression changes parallel EMT. RT-PCR assay of mRNA samples for luminal/epithelial markers (**a**), mesenchymal markers (**b**), and EMT markers (**c**) for parental MCF-7 cells (*P*), M1 through M4 mammospheres (*1–4*), two independent populations of MCF-7_M cells (*MCF-7_M*), and mesenchymal MDA-MB-231 cells (*231*), − indicates no reverse transcriptase control. GAPDH, RPL-P0, and ezrin are loading controls. Data are representative from three independent experiments. **d** Assay for markers of Basal cells. Duplicate samples from MCF-7 (*MCF-7*) and MCF-7_M cells (*MCF-7_M*), samples were analyzed using endpoint RT-PCR

staining, but apoptosis was significantly lower in the MCF-7_M tumors as compared to parental MCF-7 tumors. This demonstrates that decreased apoptosis contributed to the expansion of MCF-7_M tumors.

MicroRNAs contribute to a stable EMT phenotype

MicroRNA expression was assessed by a quantitative RT-PCR array representing 88 microRNAs previously implicated in cancer. Of these 88 microRNAs, 11 displayed a more than tenfold change over parental MCF-7 cells in at least two mammosphere samples (M2, M4) or MCF-7_M cells (Fig. 6a).

Two classes of microRNAs might contribute to mammosphere-induced EMT, by a direct role in suppressing EMT (miR-200c, miR-203, and miR-205); [20, 21, 29, 35] or by targeting ERα mRNA (miR-221/222) [36]. miR-200c, miR-203, and miR-205 were found to be decreased by 380-fold, 50-fold, and 2500-fold, respectively, in MCF-7_M cells compared to parental MCF-7 cells (Fig. 6a). These decreases were confirmed by semi-quantitative endpoint PCR (Fig. 6b). miR-200c was also repressed in MCF-7_M cell-derived tumors (Fig. 7b). The strong repression of these microRNAs further establishes that a stable EMT had occurred.

The direct suppression of ERα by specific microRNAs has been previously demonstrated [36–39], but no studies have shown an increase in ERα-targeting microRNAs during EMT. The array revealed that miR-222, known to target ERα mRNA [36], was increased more than 20-fold in MCF-7_M cells (Fig. 6a; arrow).The sustained increase in miR-222 and its bicistronic partner, miR-221, was also confirmed by endpoint PCR analysis in MCF-7_M cells (Figs. 6b, 7a), and MCF-7_M cell-derived tumors (Fig. 7b).

A functional relationship between increased miR-221 and reduced ERα was examined by treating MCF-7_M cells with antisense hairpin inhibitor. Transfection of MCF-7_M cells with antisense RNA to miR-221 increased ERα protein several-fold (Fig. 7c). This suggests that the miR-221-mediated repression of ERα mRNA contributed to the induction of a stable EMT in this system. Consistent with previous findings that miR-221 or miR-222 does not affect ERa mRNA levels [36], anti-miR-221 did not lower the level of ERa mRNA in the studies (data not shown).

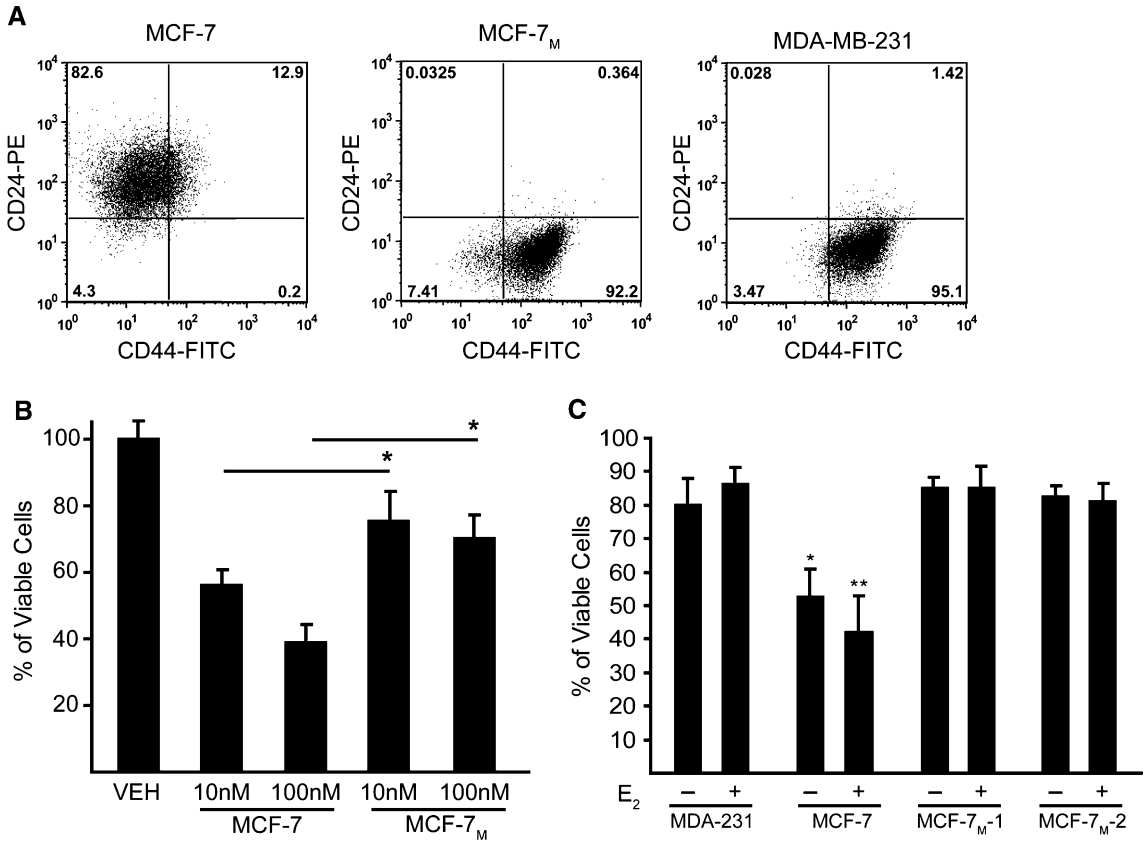

Fig. 3 MCF-7_M cells acquire a $CD44^+/CD24^{-/low}$ phenotype and display chemoresistance. **a**–**c** Flow cytometric analysis of CD24 and CD44 surface markers in MCF-7, MCF-7_M, and MDA-MB-231 cells. **b** Resistance to docetaxel. Cells were treated with 10 or 100 nM docetaxel or vehicle control (*VEH*) for 24 h and viable cells counted. *Error bars* represent the SEM for three independent experiments. Statistical significance between comparable treatments, $^*P \leq 0.05$. **c** Resistance to tamoxifen. Effects 10 μM tamoxifen, −/+1 nM E_2, on viable cell counts after 48 h. Data are presented as the percentage of viable cells in tamoxifen-treated samples compared to vehicle for each condition and cell type. *Error bars* represent the SEM for three independent experiments. Statistical significance between comparable treatments, $^*P \leq 0.05$, $^{**}P < 0.01$

Discussion

Mammosphere culture was first used to enrich for adult mammary stem cells under non-differentiating culture conditions [26]. Cells from these mammospheres were capable of self-renewal and differentiation into complex mammary tree-like structures. Subsequently, mammospheres from primary breast cancer specimens and MCF-7 cells have been generated [33]. Consistent with other reports [34], the majority of these cells were $CD44^+/CD24^{-/low}$ and highly tumorigenic. Since these landmark papers, numerous studies have utilized mammosphere culture to enrich for CSCs from primary IBC and cancer cell lines [40]. Here, we have demonstrated that prolonged mammosphere culture of MCF-7 cells ultimately generates a stable population of mesenchymal cells through an EMT process.

In support of this conclusion, we observed increased migratory capacity and proliferation rate of MCF-7_M cells, and persistent induction of EMT effector genes (Snail 1, Slug, Zeb1, Zeb2, and Axl). These effects presumably lead to the suppression of epithelial/luminal genes (ERα, E-cadherin, GATA3, claudin 3, miR-200c, miR-203, and miR-205) and increased expression of mesenchymal genes (vimentin, EGFR, α6 integrin, and moesin). MCF-7_M cells retained their mesenchymal appearance and gene expression through many passages in vitro and through tumor formation in vivo. MCF-7_M cells gave rise to tumors with reduced apoptosis, increased expansion, and estradiol independence.

Mammosphere-induced EMT is further supported by the observation that MCF-7_M cells display several features indicative of an increased CSC population. These include expansion of the $CD44^+/CD24^{-/low}$ fraction [9, 33, 34, 41], similar to the more stem-like "Basal B" subgroup [32], and increased resistance to tamoxifen and docetaxel.

Other studies have induced EMT in breast cancer cells using ectopic gene overexpression [9, 31] or uninterrupted exposure to an EMT-inducing growth factor [42]. In contrast, our model of EMT induction did not involve ectopic gene expression, and MCF-7_M cells retained their mesenchymal phenotype long after removal from mammosphere culture.

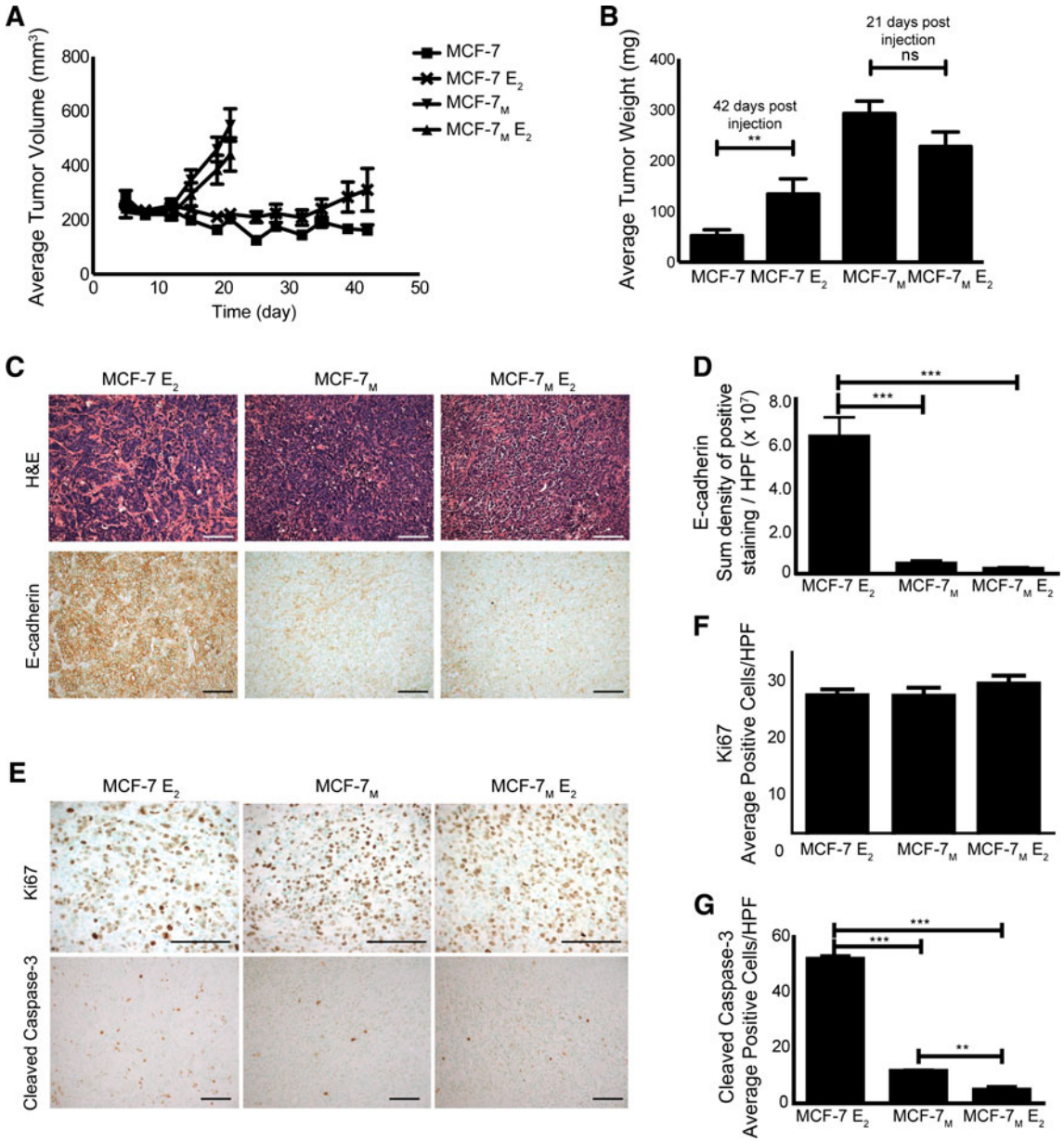

Fig. 4 MCF-7_M cells are tumorigenic in vivo and estradiol independent. **a** MCF-7 and MCF-7_M cells were injected within Matrigel matrix into SCID mice with or without E_2 supplementation. Tumor volumes were measured twice weekly and plotted over time. *Note*: MCF-7_M tumors were harvested at 21 days due to rapid growth. **b** Tumors for each group were excised and weighed at harvest ($n = 10$). **c** Histological analysis of tumors from MCF-7 and MCF-7_M injected animals. Hematoxylin and Eosin (*H&E*) stained viable tumor areas and E-cadherin staining in similar location. **d** Quantitative image analysis of E-cadherin staining in the different tumors ($n = 3$). **e** Analysis of tumor cell proliferation and apoptosis by Ki67 and cleaved caspase-3, respectively. **f** Quantitative image analysis of Ki67 staining in the different tumor groups ($n = 3$). **g** Quantitative image analysis of tumor cleaved caspase-3 staining ($n = 3$). *Bar* graphs represent average and *error bars* SEM Statistical significance for indicated comparisons, $*P \leq 0.05$, $**P \leq 0.01$, $***P \leq 0.001$

Thus, the EMT induced in the study appears to be due to a stable epigenetic switch. Such a switch was recently demonstrated in human mammary epithelial cells in response to a transient stimulus, and required the NFKB/IL-6 positive-feedback loop [43]. EMT in the study was also associated with IL-6 mRNA expression. IL-6 overexpression has been shown to induce EMT in MCF-7 cells [31], and IL-6 positive-feedback loops have been observed in lung [44] and breast cancers [45]. A threshold of IL-6 secretion may explain the apparent wave of EMT that occurred at week 3 of mammosphere culture. We speculate that growth factors in mammosphere medium (EGF, bFGF, and insulin [46–48]) induced a progressive positive-feedback loop that ultimately became self-sustaining.

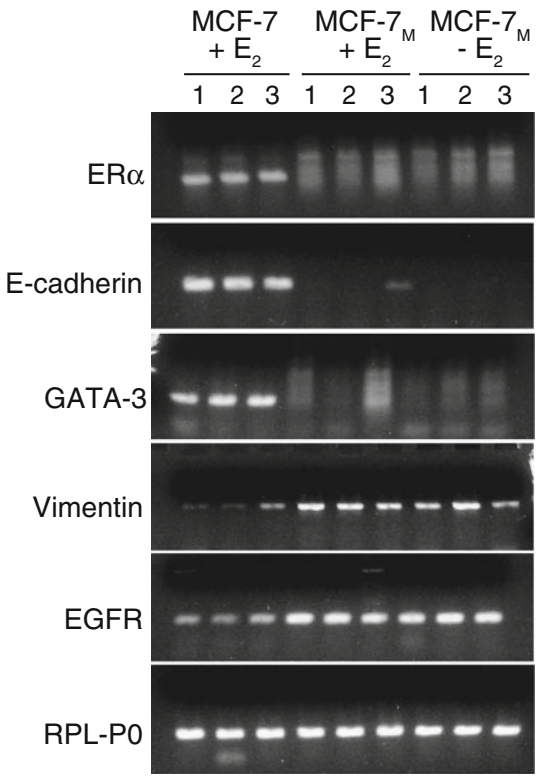

Fig. 5 MCF-7_M cells retain the mesenchymal phenotype in vivo. Total RNA was isolated from three frozen tumor samples for each group and endpoint RT-PCR from 30 cycles shown for ERα, E-cadherin, GATA-3, vimentin, EGFR, and control RPL-P0

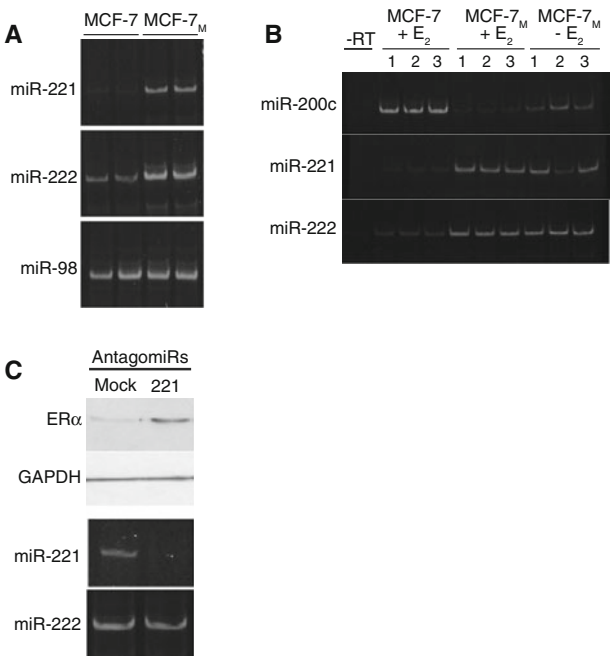

Fig. 7 ERα is downregulated by ERα-targeting microRNAs in MCF-7_M cells. ERα-inhibitory microRNAs miR-221 and miR-222 are increased in MCF-7_M cells (**a**), and maintained expression in tumors (**b**). **c** miRIDIAN^{TM} microRNA hairpin inhibitor to miR-221 induced ERα protein expression in MCF-7_M cells. GAPDH is a loading control

ERα represses Snail 1 and Slug expression [13, 14], and GATA3 blocks or reverses EMT in MDA-MB-231 cells [17]. Thus, unlike EMT in other cancers, EMT in luminal breast cancers must involve a breach of the EMT-opposing actions of ERα and GATA3. We found massive increases in miR-221/miR-222 that might account for such a breach. Consistent with this model, miRs-221/222 are upregulated in ERα-negative breast cancers and directly target sites within the 3′ UTR of ERα mRNA [36]. miRs-221/222 were

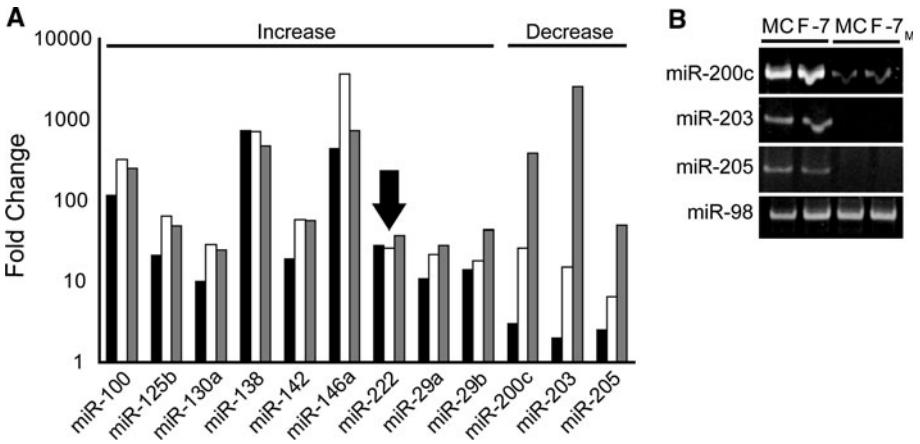

Fig. 6 EMT-induced changes in microRNA expression. **a** Results from four "Cancer microRNA" RT^2 microRNA PCR arrays performed on parental MCF-7 cells, M2 and M4 mammospheres, and MCF-7_M cell RNA samples. Values are presented as fold-change (increased, *left*; decreased, *right*) in the latter three groups relative to parental MCF-7 cells (note log scale). MicroRNAs from the array that showed $a >$ tenfold change in at least two of the three samples are shown except for miR-205 (M2, *black*; M4, *white*; MCF-7_M, *gray*). *Solid arrow* points out miR-222. **b** EMT suppressed epithelial-associated microRNAs, miR-220c, miR-203, and miR-205. RT-PCR of miR-98 (loading control), miR-200c, miR-203, and miR-205 performed in duplicate on RNA samples from MCF-7 and MCF-7_M cells which validate the PCR array results

elevated in tamoxifen-resistant MCF-7 cells and Her-2-positive breast cancer, and ectopic expression of miRs-221/222 conferred tamoxifen-resistance to MCF-7 cells [45]. The anti-estrogen Fulvestrant induced miR-221/222 expression that was essential for the growth of fulvestrant–resistant cells [49].

Zhao et al. [36] demonstrated that anti-miR-221 and anti-miR-222 induced the appearance of detectable ERα protein in MDA-MB-468 and MCF10A cells, in which ERα mRNA is normally present. Similarly, MCF-7_M cells display barely detectable ERα protein and mRNA levels. The finding that treatment of MCF-7_M cells with antisense hairpin RNA against miR-221 induced a large increase in ERα protein indicates that miR-221 reduces ERα expression MCF-7_M cells. Thus, in luminal IBC, EMT and loss of ERα expression could be linked, through transcriptional repression of ERα by Snail, and concomitant translational inhibition of ERα mRNA by miR-221/222. Since ERα antagonizes EMT through GATA3 and FOXA1, this loss of ERα would ultimately remove further blocks to EMT.

In summary, serial mammosphere culture of MCF-7 cells induced a persistent EMT and generated a population of cells with several properties of CSCs. Unlike most cancers, EMT in epithelial (luminal A) IBC is associated with reduced ERα signaling, and we show herein that specific microRNAs that target ERα are stably upregulated during EMT. We anticipate that mammosphere-induced EMT will be a useful model to study interactions between ERα signaling, EMT, and expansion of CSCs within a tumor, as well as other aspects of cancer-associated EMT mechanisms.

Acknowledgments We wish to thank Dr. Lisa Mehlmann, Department of Cell Biology, UCHC, for her assistance with microscopy. Financial support is from R21 DK073456, NIH/NIDDK (BW); NIH/NCI CA064436 (KPC).

References

1. Prat A, Parker JS, Karginova O, Fan C, Livasy C, Herschkowitz JI, He X, Perou CM (2010) Phenotypic and molecular characterization of the claudin-low intrinsic subtype of breast cancer. Breast Cancer Res 12:R68
2. Bertucci F, Finetti P, Cervera N, Charafe-Jauffret E, Buttarelli M, Jacquemier J, Chaffanet M, Maraninchi D, Viens P, Birnbaum D (2009) How different are luminal A and basal breast cancers? Int J Cancer 124:1338–1348
3. Kalluri R, Weinberg RA (2009) The basics of epithelial-mesenchymal transition. J Clin Invest 119:1420–1428
4. Micalizzi DS, Farabaugh SM, Ford HL (2010) Epithelial-mesenchymal transition in cancer: parallels between normal development and tumor progression. J Mammary Gland Biol Neoplasia 15:117–134
5. Zeisberg M, Neilson EG (2009) Biomarkers for epithelial-mesenchymal transitions. J Clin Invest 119:1429–1437
6. Nadella KS, Jones GN, Trimboli A, Stratakis CA, Leone G, Kirschner LS (2008) Targeted deletion of Prkar1a reveals a role for protein kinase A in mesenchymal-to-epithelial transition. Cancer Res 68:2671–2677
7. Polyak K, Weinberg RA (2009) Transitions between epithelial and mesenchymal states: acquisition of malignant and stem cell traits. Nat Rev Cancer 9:265–273
8. Thiery JP, Acloque H, Huang RY, Nieto MA (2009) Epithelial-mesenchymal transitions in development and disease. Cell 139:871–890
9. Mani SA, Guo W, Liao MJ, Eaton EN, Ayyanan A, Zhou AY, Brooks M, Reinhard F, Zhang CC, Shipitsin M, Campbell LL, Polyak K, Brisken C, Yang J, Weinberg RA (2008) The epithelial-mesenchymal transition generates cells with properties of stem cells. Cell 133:704–715
10. Singh A, Settleman J (2010) EMT, cancer stem cells and drug resistance: an emerging axis of evil in the war on cancer. Oncogene 29:4741–4751
11. Blick T, Hugo H, Widodo E, Waltham M, Pinto C, Mani SA, Weinberg RA, Neve RM, Lenburg ME, Thompson EW (2010) Epithelial mesenchymal transition traits in human breast cancer cell lines parallel the CD44(hi/)CD24 (lo/-) stem cell phenotype in human breast cancer. J Mammary Gland Biol Neoplasia 15:235–252
12. Creighton CJ, Chang JC, Rosen JM (2010) Epithelial-mesenchymal transition (EMT) in tumor-initiating cells and its clinical implications in breast cancer. J Mammary Gland Biol Neoplasia 15:253–260
13. Ye Y, Xiao Y, Wang W, Yearsley K, Gao JX, Shetuni B, Barsky SH (2010) ERα signaling through slug regulates E-cadherin and EMT. Oncogene 29:1451–1462
14. Fujita N, Jaye DL, Kajita M, Geigerman C, Moreno CS, Wade PA (2003) MTA3, a Mi-2/NuRD complex subunit, regulates an invasive growth pathway in breast cancer. Cell 113:207–219
15. Eeckhoute J, Keeton EK, Lupien M, Krum SA, Carroll JS, Brown M (2007) Positive cross-regulatory loop ties GATA-3 to estrogen receptor alpha expression in breast cancer. Cancer Res 67:6477–6483
16. Dydensborg AB, Rose AA, Wilson BJ, Grote D, Paquet M, Giguere V, Siegel PM, Bouchard M (2009) GATA3 inhibits breast cancer growth and pulmonary breast cancer metastasis. Oncogene 28:2634–2642
17. Yan W, Cao QJ, Arenas RB, Bentley B, Shao R (2010) GATA3 inhibits breast cancer metastasis through the reversal of epithelial-mesenchymal transition. J Biol Chem 285:14042–14051
18. Song Y, Washington MK, Crawford HC (2010) Loss of FOXA1/2 is essential for the epithelial-to-mesenchymal transition in pancreatic cancer. Cancer Res 70:2115–2125
19. Creighton CJ, Li X, Landis M, Dixon JM, Neumeister VM, Sjolund A, Rimm DL, Wong H, Rodriguez A, Herschkowitz JI, Fan C, Zhang X, He X, Pavlick A, Gutierrez MC, Renshaw L, Larionov AA, Faratian D, Hilsenbeck SG, Perou CM, Lewis MT, Rosen JM, Chang JC (2009) Residual breast cancers after conventional therapy display mesenchymal as well as tumor-initiating features. Proc Natl Acad Sci USA 106:13820–13825
20. Brabletz S, Brabletz T (2010) The ZEB/miR-200 feedback loop–a motor of cellular plasticity in development and cancer? EMBO Rep 11:670–677
21. Dykxhoorn DM (2010) MicroRNAs and metastasis: little RNAs go a long way. Cancer Res 70:6401–6406
22. Greene RM, Pisano MM (2010) Palate morphogenesis: current understanding and future directions. Birth Defects Res C 90:133–154
23. de Herreros AG, Peiro S, Nassour M, Savagner P (2010) Snail family regulation and epithelial mesenchymal transitions in breast cancer progression. J Mammary Gland Biol Neoplasia 15:135–147

24. O'Day E, Lal A (2010) MicroRNAs and their target gene networks in breast cancer. Breast Cancer Res 12:201
25. Charafe-Jauffret E, Ginestier C, Iovino F, Wicinski J, Cervera N, Finetti P, Hur MH, Diebel ME, Monville F, Dutcher J, Brown M, Viens P, Xerri L, Bertucci F, Stassi G, Dontu G, Birnbaum D, Wicha MS (2009) Breast cancer cell lines contain functional cancer stem cells with metastatic capacity and a distinct molecular signature. Cancer Res 69:1302–1313
26. Dontu G, Abdallah WM, Foley JM, Jackson KW, Clarke MF, Kawamura MJ, Wicha MS (2003) In vitro propagation and transcriptional profiling of human mammary stem/progenitor cells. Genes Dev 17:1253–1270
27. Varkonyi-Gasic E, Wu R, Wood M, Walton EF, Hellens RP (2007) Protocol: a highly sensitive RT-PCR method for detection and quantification of microRNAs. Plant Methods 3:12
28. Phoenix KN, Vumbaca F, Fox MM, Evans R, Claffey KP (2010) Dietary energy availability affects primary and metastatic breast cancer and metformin efficacy. Breast Cancer Res Treat 123: 333–344
29. Greene SB, Herschkowitz JI, Rosen JM (2010) The ups and downs of miR-205: identifying the roles of miR-205 in mammary gland development and breast cancer. RNA Biol 7:300–304
30. Gjerdrum C, Tiron C, Hoiby T, Stefansson I, Haugen H, Sandal T, Collett K, Li S, McCormack E, Gjertsen BT, Micklem DR, Akslen LA, Glackin C, Lorens JB (2010) Axl is an essential epithelial-to-mesenchymal transition-induced regulator of breast cancer metastasis and patient survival. Proc Natl Acad Sci USA 107:1124–1129
31. Sullivan NJ, Sasser AK, Axel AE, Vesuna F, Raman V, Ramirez N, Oberyszyn TM, Hall BM (2009) Interleukin-6 induces an epithelial-mesenchymal transition phenotype in human breast cancer cells. Oncogene 28:2940–2947
32. Neve RM, Chin K, Fridlyand J, Yeh J, Baehner FL, Fevr T, Clark L, Bayani N, Coppe JP, Tong F, Speed T, Spellman PT, De Vries S, Lapuk A, Wang NJ, Kuo WL, Stilwell JL, Pinkel D, Albertson DG, Waldman FM, McCormick F, Dickson RB, Johnson MD, Lippman M, Ethier S, Gazdar A, Gray JW (2006) A collection of breast cancer cell lines for the study of functionally distinct cancer subtypes. Cancer Cell 10:515–527
33. Ponti D, Costa A, Zaffaroni N, Pratesi G, Petrangolini G, Coradini D, Pilotti S, Pierotti MA, Daidone MG (2005) Isolation and in vitro propagation of tumorigenic breast cancer cells with stem/progenitor cell properties. Cancer Res 65:5506–5511
34. Al-Hajj M, Wicha MS, Benito-Hernandez A, Morrison SJ, Clarke MF (2003) Prospective identification of tumorigenic breast cancer cells. Proc Natl Acad Sci USA 100:3983–3988
35. Shimono Y, Zabala M, Cho RW, Lobo N, Dalerba P, Qian D, Diehn M, Liu H, Panula SP, Chiao E, Dirbas FM, Somlo G, Pera RA, Lao K, Clarke MF (2009) Downregulation of miRNA-200c links breast cancer stem cells with normal stem cells. Cell 138: 592–603
36. Zhao JJ, Lin J, Yang H, Kong W, He L, Ma X, Coppola D, Cheng JQ (2008) MicroRNA-221/222 negatively regulates estrogen receptor alpha and is associated with tamoxifen resistance in breast cancer. J Biol Chem 283:31079–31086
37. Adams BD, Cowee DM, White BA (2009) The role of miR-206 in the epidermal growth factor (EGF) induced repression of estrogen receptor-alpha (ERα) signaling and a luminal phenotype in MCF-7 breast cancer cells. Mol Endocrinol 23:1215–1230
38. Adams BD, Furneaux H, White BA (2007) The micro-ribonucleic acid (miRNA) miR-206 targets the human estrogen receptor-alpha (ERα) and represses ERα messenger RNA and protein expression in breast cancer cell lines. Mol Endocrinol 21: 1132–1147
39. Spizzo R, Nicoloso MS, Lupini L, Lu Y, Fogarty J, Rossi S, Zagatti B, Fabbri M, Veronese A, Liu X, Davuluri R, Croce CM, Mills G, Negrini M, Calin GA (2010) miR-145 participates with TP53 in a death-promoting regulatory loop and targets estrogen receptor-alpha in human breast cancer cells. Cell Death Differ 17:246–254
40. Charafe-Jauffret E, Ginestier C, Birnbaum D (2009) Breast cancer stem cells: tools and models to rely on. BMC Cancer 9:202
41. Taube JH, Herschkowitz JI, Komurov K, Zhou AY, Gupta S, Yang J, Hartwell K, Onder TT, Gupta PB, Evans KW, Hollier BG, Ram PT, Lander ES, Rosen JM, Weinberg RA, Mani SA (2010) Core epithelial-to-mesenchymal transition interactome gene-expression signature is associated with claudin-low and metaplastic breast cancer subtypes. Proc Natl Acad Sci USA 107:15449–15454
42. Fuxe J, Vincent T, de Herreros AG (2010) Transcriptional crosstalk between TGFβ and stem cell pathways in tumor cell invasion: role of EMT promoting Smad complexes. Cell Cycle 9: 2363–2374
43. Iliopoulos D, Hirsch HA, Struhl K (2009) An epigenetic switch involving NF-kappaB, Lin28, Let-7 microRNA, and IL6 links inflammation to cell transformation. Cell 139:693–706
44. Gao SP, Mark KG, Leslie K, Pao W, Motoi N, Gerald WL, Travis WD, Bornmann W, Veach D, Clarkson B, Bromberg JF (2007) Mutations in the EGFR kinase domain mediate STAT3 activation via IL-6 production in human lung adenocarcinomas. J Clin Invest 117:3846–3856
45. Sansone P, Storci G, Tavolari S, Guarnieri T, Giovannini C, Taffurelli M, Ceccarelli C, Santini D, Paterini P, Marcu KB, Chieco P, Bonafe M (2007) IL-6 triggers malignant features in mammospheres from human ductal breast carcinoma and normal mammary gland. J Clin Invest 117:3988–4002
46. Lo HW, Hsu SC, Xia W, Cao X, Shih JY, Wei Y, Abbruzzese JL, Hortobagyi GN, Hung MC (2007) Epidermal growth factor receptor cooperates with signal transducer and activator of transcription 3 to induce epithelial-mesenchymal transition in cancer cells via up-regulation of TWIST gene expression. Cancer Res 67:9066–9076
47. Wu X, Chen H, Parker B, Rubin E, Zhu T, Lee JS, Argani P, Sukumar S (2006) HOXB7, a homeodomain protein, is overexpressed in breast cancer and confers epithelial-mesenchymal transition. Cancer Res 66:9527–9534
48. Zhau HE, Odero-Marah V, Lue HW, Nomura T, Wang R, Chu G, Liu ZR, Zhou BP, Huang WC, Chung LW (2008) Epithelial to mesenchymal transition (EMT) in human prostate cancer: lessons learned from ARCaP model. Clin Exp Metastasis 25:601–610
49. Rao X, Di Leva G, Li M, Fang F, Devlin C, Hartman-Frey C, Burow ME, Ivan M, Croce CM, Nephew KP (2010) MicroRNA-221/222 confers breast cancer fulvestrant resistance by regulating multiple signaling pathways. Oncogene 30:1082–1097